Geometrical Data analysis
Singer Gabriel
Membrane and tubular shape generation, from theory to practice

1 INTRODUCTION

Quantitative medicine has been booming since the 2000s, thanks in part to its computational and data-processing capabilities. It interests mathematicians [15], physicians [11], physicists [16], and also biologists [2, 12].As a result of this kind of collaboration is Song's article [1], mixing theoretical mathematics, and computer science. Its results have applications in materials science and especially in the study of blood vessels and blood cancer.

Depending on the scale you look at a biological shape, a lot of shapes can be seen as membranous or tubular.

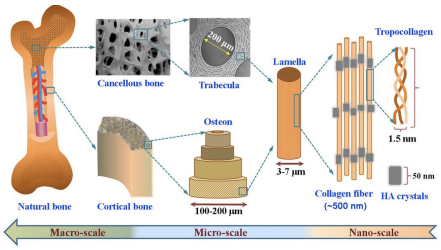

Figure 1: Human bones seen at different scales, [17]

The modeling of tubular and membranous shapes represents a major medical challenge.

In fact, the topological shape of a biological system tells us a lot of information about its condition, and enables us, among other things, to see how it reacts to certain treatments, [22].

For example, our kidneys are full of porous, tube-shaped structures. These are called RTCs for "Renal Tubular Cells" [23, 29]. Because of their topological complexity (many holes, irregularities, complex shapes), there is no complet general theory to describe them.

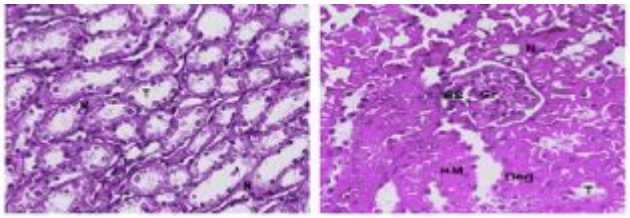

Figure 2: Rat renal cells, [22]

Song's paper [1] proposes an effective generative model for generating biological and mechanical structures :

This model generalizes numerous works [14, 15, 21].

Conference'17, July 2017, Washington, DC, USA
2023. ACM ISBN 978-x-xxxx-xxxx-x/YY/MM…$15.00
https://doi.org/10.1145/nnnnnnn.nnnnnnn

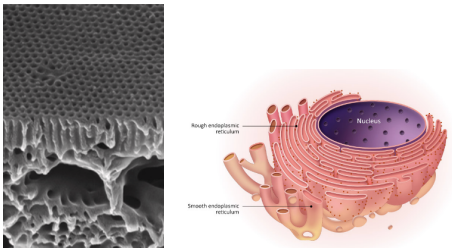

Figure 3: Left: Polymer structure. Right: endoplasmic reticulum

This article is part of a much larger project undertaken by the author. This paper takes a qualitative rather than quantitative approach, which I believe will have a greater impact in the years to come. The first is to be able to generate these tubular shapes. The second is to quantify texture using algebraic topology. More specifically, using homological persistence. And the third looks at data extraction in practice.

We begin with the theoretical part, with the statement of the main theorem, and then turn to some of the numerical aspects developed in this article.

1.1 Theoritical part

From a theoretical point of view, A.Song models the S shape as an optimum of the curvature functional:

$$F(S) = \int_S p(k_1, k_2) dA, \quad p \in \mathbb{R}[X, Y] \tag{1}$$

and k_1 and k_2 are the principal curvatures of S.

We write

$$p(k_1, k_2) = \sum_{|\alpha| \leq 2} a_\alpha (k_1, k_2)^\alpha.$$

Note that the functional (1) where p is a function more general than a polynomial is studied in [18, 20].

Historically, the first functional that was considered was :

$$F(S) = \int_S \mathbb{I} dA$$

and you minimize it over an admissible class of sets you get the sphere. This is also very close to the isoperimetric problem where you are looking for the biggest volume for a given perimeter and if you choose a sufficiently compact class of sets you get as optimum a sphere.

This is actually a good model to explain the shape of bubble swoap !

Then, in the 1960's Willemore introduced

$$W = \int_S H^2 dS \quad \text{where} \quad H = \kappa_1 + \kappa_2.$$

And approximately 10 years later, Helfrich introduced

$$H(S) = \int_S \frac{\chi_b}{2}(H - H_0)^2 + \chi_G k dA.$$

H presents global minimum. These minimums depends on the genus, noted g we consider. If $g = 0$ it has been demonstrated that the minimum is a sphere, for $g = 1$ it is the Clifford torus, and for $g \geq 2$ the question is still open. It is conjectured that for $g = 2$ the flow converges to a Lawson-like surface.

Numerrically the case $g = 1, 2, 3$ are investigated :

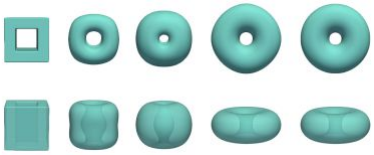

Figure 4: Convergence of the flow in the case of $g = 1$, [1]

However, from a numerical point of view, the formula (1) is not very practical to use, because, among other things, it's complicated to adapt the mesh as S varies. The idea is to introduce a functionnam that depends on $u : \Omega \subset \mathbb{R}^3 \to \mathbb{R}$ and see S as the cancellation points of u.

A way to study the above functional is to introduce a family of functional $(F_\varepsilon)_\varepsilon$ which, in a sense, approximate F. This point of view comes from the field of geometrical measur theory where Villani, De Giorgi and Maggi are mathematician very involved in this field. A very good book about link between shape optimization and measure theory are [25, 26].

Actually the Γ convergence ensures that if we know how to find an optimum x_ε at F_ε then for a certain metric $\lim_\varepsilon x_\varepsilon = x$ where x is an optimum of F where F is the Γ limit of $(F_\varepsilon)_\varepsilon$. This subject is covered in detail in topological form optimization, [25].

More rigorously, we define

Definition 1 (Γ-convergence). *Given X a metric space, let F and F_ε be functions from X to $[-\infty, +\infty]$, where the F_ε are defined for $\varepsilon > 0$. We say that the sequence $(F_\varepsilon)_{\varepsilon>0}$ Γ-converges to F at a point $u \in X$ as $\varepsilon \to 0$, and write*

$$[\Gamma(X) - \lim_{\varepsilon \to 0} F_\varepsilon](u) = F(u),$$

if the following two bounds hold: [Γ-liminf] For every sequence (u_ε) such that $u_\varepsilon \to u$ in X,

$$\liminf_{\varepsilon \to 0} F_\varepsilon(u_\varepsilon) \geq F(u).$$

[Γ-limsup] There exists a sequence (u_ε), called a recovery sequence, such that $u_\varepsilon \to u$ in X and

$$\lim_{\varepsilon \to 0} F_\varepsilon(u_\varepsilon) = F(u).$$

and then we have the theorem that makes the link :

Theorem 1. *Let X be a metric space, and let $F = \Gamma(X)\text{–}\lim_{\epsilon \to 0} F_\epsilon$. Suppose that the sequence $F_\epsilon : X \to [-\infty, +\infty]$ is equi-coercive, i.e., for all $t \in \mathbb{R}$, there exists a compact set $K_t \subset X$ such that $\{F_\epsilon \leq t\} \subset K_t$. Then F admits a minimum, and*

$$\min_X F = \lim_{\epsilon \to 0} \inf_X F_\epsilon.$$

Furthermore, if u_ϵ minimizes F_ϵ over X, then every cluster point of (u_ϵ) minimizes F over X.

Γ convergence are very hard questions, for instance, for a very less complicated formulation of $(F_\varepsilon)_\varepsilon$, the Cahn-Hillard phase field, the the Γ convergenc is given by a conjecture of De Giorgi, Modica, and Mortola [30]. However, Bellettini and Paolini [31] introduced the phase-fields

$$W_\varepsilon(u) = \begin{cases} \frac{1}{\varepsilon}\int_\Omega (\varepsilon\Delta u - W_0(u))^2 \, dx & \text{if } u \in W^{2,2}(\Omega), \\ +\infty & \text{otherwise in } L^1(\Omega). \end{cases}$$

Finally, Bellettini and Mugnai [6] extended the Willmore phase-field to approximate the complete Helfrich energy with

$$H_\varepsilon(u) = \begin{cases} \int_\Omega \left(\frac{\chi_b^2}{2\varepsilon}\varepsilon(TrM_u^\varepsilon - \varepsilon|\nabla u|H_0)^2 + \right. & \\ \left. \frac{\chi_G^2}{2\varepsilon}(TrM_u^\varepsilon)^2 - ||M_u^\varepsilon||^2 \, dx \right. & \text{if } u \in C^2(\Omega), \\ +\infty & \text{otherwise in } L^1(\Omega). \end{cases}$$

They proved, thanks to the previous results of R¨oger and Sch¨atzle [32], and under some technical assumption that they showed that Γ-convergence holds on smooth points

$u = 2\chi_E 1$ where $E \subset \Omega$ is open and $\partial E \cap \Omega \in C$.

And finally, to generalize the previous phase field, Song introduces the functional F_ε:

$$\begin{aligned} F_\varepsilon(u) = \int_\Omega & \frac{a_{2,0} + a_{0,2} - a_{1,1}}{2\epsilon} \left\|M_u^\varepsilon\right\| + \frac{a_{1,1}}{2\epsilon}\left(\mathrm{Tr}M_u^\varepsilon\right)^2 \\ & + \frac{a_{2,0} - a_{0,2}}{2\epsilon}\mathrm{Tr}(M_u^\varepsilon)\sqrt{(2\,||M_u^\varepsilon||^2 - (\mathrm{Tr}M_u^\varepsilon)^2)^+} + \\ & \frac{a_{1,0} + a_{0,1}}{2}|\nabla u|\mathrm{Tr}(M_u^\varepsilon) \\ & + \frac{a_{1,0} - a_{0,1}}{2}|\nabla u|\sqrt{(2\,||M_u^\varepsilon||^2 - (\mathrm{Tr}M_u^\varepsilon)^2)^+} + a_{0,0}\epsilon|\nabla u|^2 d\sigma \quad (\star) \end{aligned}$$

Where, for a given function u twice weakly differentiable, we define the normal vector field $\mathbf{n}_u$ as:

$$\mathbf{n}_u = \begin{cases} \frac{\nabla u}{|\nabla u|} & \text{on the set } \{\nabla u \neq 0\} \\ \mathbf{e} & \text{elsewhere} \end{cases}$$

where $\mathbf{e}$ represents any vector in the absence of ∇u. This field has unit norm and is orthogonal to the level sets of u.

Where the matrix field M_u^ε is defined as:

$$M_u^\varepsilon = -\epsilon\nabla^2 u + \frac{W(u)}{\epsilon}\mathbf{n}_u \otimes \mathbf{n}_u$$

whose trace is equal to:

$$\mathrm{Tr}M_u^\varepsilon = -\epsilon\Delta u + \frac{W(u)}{\epsilon}$$

With

$$W : u \mapsto \frac{(1 - u^2)^2}{2}.$$

The main theorem of this paper is :

Theorem 2 (Γ-limsup inequality, [1]). *Let $E \subset \Omega$ be a bounded open set, such that $\partial E \cap \Omega$ is of class C^2. The functionals F_ε and F are*

defined as in (⋆) and (1). Then, there exists a sequence of functionals $(u_\varepsilon)_{\varepsilon>0} \subset W^{2,2}(\Omega)$ *such that*

$$\lim_{\varepsilon\to 0+} u_\varepsilon = 2\chi_E - 1 \quad in\ L^1(\Omega), \tag{2}$$

$$\lim_{\varepsilon\to 0+} |\nabla u_\varepsilon|^2 |\mathcal{L}^3() = \sigma\mathcal{H}^2|\partial E \text{ as Radon measures}, \tag{3}$$

$$\lim_{\varepsilon\to 0+} F_\varepsilon(u_\varepsilon) = \sigma F(E). \tag{4}$$

Since, if you choose

$$a = (\chi_b^2, \chi_b + \chi_G, \chi_b^2, -\chi_b H_0, -\chi_b H_0, \chi_b^2 H_0^2)$$

we get for F_ε the functional defined and studied by Bellettini and Mugnai in [21], one can see that this theorem generalizes the Γ limit inf result stated by [21] without the need for a finite perimeter assumption and $H_0 = 0$ but at the cost of not having Γ convergence.

Then, taking $p(\kappa_1, \kappa_2) = H^2$ which is

$$a = (1, 2, 1, 0, 0, 0)$$

we find the Willmore functional, [13].

This result is in line with the notion of Γ functional convergence.

The question of the Γ limit inf for the functional F_ε as defined in [1] by Song is still open, except for the special cases already studied [21].

1.2 Numerical part

The numerical part of Song's article is a major generalization of many previous works. In fact, in numerous articles [14–16], the authors focus on the simulation associated with the Cahn-Hilliard functional in 2 dimension.

Here, Song proposes an algorithm to obtain surfaces immersed in $\mathbb{R}^3$, which makes things even more realistic.

Level-set methods were introduced by Osher and Sethian (1988).

The level set method consists of representing a surface $S \subset \mathbb{R}^3$ by

$$S := \left\{x \in \mathbb{R}^3 \quad u(x) = 0\right\}.$$

Où pour H un espace de Hilbert, $\tilde{u}$ dépend du temps et est telle que

$$\lim_{t\to\infty} ||u - \tilde{u}||_H = 0$$

et $\tilde{u}$ verifie

$$\partial_t \tilde{u} = -\frac{\partial F}{\partial \tilde{u}}, \quad \tilde{u}(x,0) = \phi_0(x) \tag{5}$$

tandis que u est solution de l'équation stationnaire ;

$$\frac{\partial F}{\partial u}(u) = 0.$$

We recall that, for a for a functional $F : H \to \mathbb{R}$, where H is an Hilbert space, we define $\partial_u F$ as the unique $w \in H$ veryfing

$$(F'(u), v)_H = (w, v)_H, \quad \forall v \in H$$

where

$$\lim_{t\to 0} \frac{F(u+tv) - F(u)}{t} = (F'(u), v)_H \quad \forall v \in C_c^\infty(\Omega).$$

The school case (which is a particular case of [1] for $P = a_{00} > 0$) is that of the Dirichlet problem where $H = L^2(\Omega)$ and $F_\varepsilon : u \mapsto a_{00}\varepsilon\, ||\nabla u||_{L^2(\Omega)}$. In this cas we have :

$$\partial_u F_\varepsilon : u \mapsto -2a_{00}\varepsilon\Delta u,$$

where the $L^2(\Omega)$ flow is

$$\partial_t u = 2a_{00}\varepsilon\Delta u \tag{6}$$

We can also study for $\varepsilon = 1$ the Cahn-Hillard functionnal

$$F : u \mapsto \frac{1}{2}\int_\Omega |\nabla u(x)|^2 + W(u(x))dx, \quad W \in C^\infty$$

On $L^2(\Omega)$

$$\partial_u F : u \mapsto -2\Delta u + W'(u) \tag{7}$$

In fact, let $v \in C_c^\infty(\Omega)$ and $u \in L^2(\Omega)$ then, for any $t > 0$ we have that

$$\frac{F(u+tv) - F(u)}{t} = \frac{t}{2}\int_\Omega |\nabla v(x)|^2\, dx + \int_\Omega \nabla u(x)\nabla v(x)dx + \int_\Omega \frac{W(u(x)+tv(x)) - W(u(x))}{t}dx$$

By integrating by part (the boundary terms are nul, since v is compactly supported) we find that

$$\int_\Omega \nabla u \nabla v = -\int_\Omega \Delta u v = (-\Delta u; v)_{L^2(\Omega)}$$

plus

$$\lim_{t\to 0} t\int_\Omega |\nabla v|^2\, d\lambda = 0.$$

By the dominated convergence theorem :

$$\lim_{t\to 0}\int_\Omega \frac{W(u(x)+tv(x)) - W(u(x))}{t}dx = (v, W'(u))_{L^2}$$

This shows (7).

From the definition of $\partial_u F$ we can see that the space on which we place ourselves plays a role. The aim is for (5) to become a purely local differential equation so that it can then be solved by finite difference, for example.

The problem is that in general the equation (5) loses its locacle character, so the "right" space to consider is the dual of $H^1(\Omega)$, i.e. $H^{-1}(\Omega)$.

In which case, using the example above, the associated flow equation in $H^{-1}(\Omega)$ is written as :

$$\partial_t u = \Delta^2 u - \Delta W'(u) \tag{8}$$

This gives us the Cahn-Hilliard equation (in the case of $varepsilon = 1$).

In [1], the author considere $H^{-1}(\Omega)$-flow

$$\partial_t u = \Delta\frac{\partial F_\varepsilon}{\partial u} \tag{9}$$

which becomes L^2-flow by setting $u = Div(A) + m_0$ where $A : \Omega \mapsto \mathbb{R}$ and $m_0 \in]0,1[$ Let, $G_\varepsilon(A) := F_\varepsilon(Div(A) + m_0)$: then we get :

$$\partial_t A = -\frac{\partial G_\varepsilon}{\partial A} \quad A(0,x) = A_0.$$

From an algorithmic point of view, we're trying to implement algorithm number 1 from Song's article, [1]. With the difference that we didn't use Pytorch, we first comput manually $\partial_\varepsilon F_\varepsilon$ and we used finite difference schemes. The results we obtained are really really not as good as those obtained by Song's algorithms.

Once a shape has been obtained, Song turns her attention to quantifying its texture. To do this, she uses the curvature diagram. The texture of a shape (defined by a surface S) is quantified through

Algorithm 1 Curvatubes

procedure CURVATUBES(A_0, a, m_0)
  Initialization: Random vector field A_0
  Generation parameters: Coefficients $a = (a_{2,0}, a_{1,1}, a_{0,2}, a_{1,0}, a_{0,1}, a_{0,0})$, mass $m_0 \in (-1, 1)$
  Energy: Phase-field energy F_ε to approximate $\int_S \sum_{|\alpha|\leq 2} a_\alpha(\kappa_1, \kappa_2)\alpha \, dA$
  Other parameters: Phase transition parameter $\varepsilon > 0$, internal parameters for Adam (learning rate, betas, weight decay), number of iterations T, Gaussian kernel of size σ_k
  Outputs: Phase-field u and surface $S = \{u = 0\}$
  $A \leftarrow A_0$ ▷ Initialization of the vector field
  for $t = 1$ to T **do**
    $u \leftarrow \nabla \cdot A + m_0$ ▷ Change of variable (24)
    $u \leftarrow k * u$ ▷ Small blur to avoid artifacts
    Set $G^\varepsilon(A) := F^\varepsilon(u)$
    Compute $\frac{\partial G^\varepsilon}{\partial A}$ ▷ PyTorch autograd
    Update moments of the gradients ▷ Adam
    Update A with one step of $\dot{A} = -\frac{\partial G^\varepsilon}{\partial A}$ ▷ Adam
    $S \leftarrow \{u = 0\}$ ▷ Visualize the shape texture
  end for
end procedure

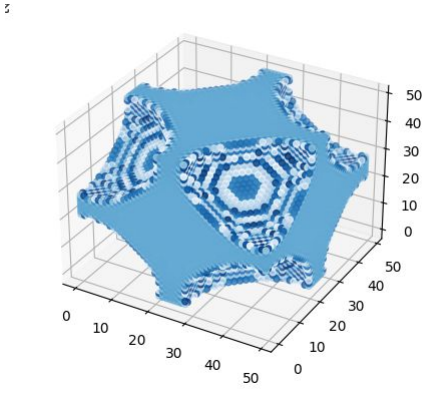

Figure 5: $\partial_t \phi = 0.7 * \Delta\phi - 0.001 * div(\phi)$

its curvature diagram. It represents the distribution of the curvatures (κ_1, κ_2) on S. The object of interest is the law of the random variable (κ_1, κ_2) defined by

$$P[(\kappa_1, \kappa_2) \in B] = \frac{\text{Area}(\{x \in S \mid (\kappa_1, \kappa_2)(x) \in B\})}{\text{Area}(S)}, \qquad (10)$$

for a Borel set B of $\mathbb{R}^2$. In a simple case, what does the probability law look like?

Let's take the sphere of radius R and B be a Borel set of $\mathbb{R}^2$. Denote $\mathbb{S}_R$ the sphere of radius $R > 0$. Since the two principal curvatures of a sphere are equal to $\frac{1}{R}$ we have that if $(x, y) \in \mathbb{S}_R$ then $k_1(x, y) = k_2(x, y) = \frac{1}{R}$ thus the support is equal to $\left\{(x, y) \in \mathbb{R}^2 \quad x = y, x > 0\right\}$ and :

$$\{u = (x, y) \in \mathbb{S}_R \quad (k_1(u), k_2(u)) \in B\} = \left\{u \in \mathbb{S}_R \quad (\frac{1}{R}, \frac{1}{R}) \in B\right\}$$

is empty if $B \neq \left\{(\frac{1}{R}, \frac{1}{R})\right\}$ and is equale to $\mathbb{S}_R$ if $B = \left\{(\frac{1}{R}, \frac{1}{R})\right\}$. Plugging it into (10) and it gives you that

$$P[(\kappa_1, \kappa_2) \in B] = \begin{cases} 0 & \text{if } (\frac{1}{R}, \frac{1}{R}) \notin B \\ 1 & \text{if } (\frac{1}{R}, \frac{1}{R}) \in B \end{cases} = \delta_{(\frac{1}{R}, \frac{1}{R})}.$$

This is exactly what we see on the diagrame curvatures constructed by Song's algorithm: You can see that the points are near

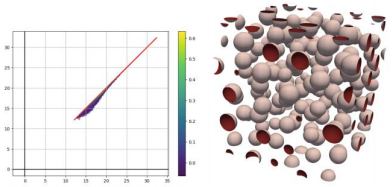

Figure 6: Points $(\kappa_1; \kappa_2)$, from [1].

to the red line $y = x$ which means that $\kappa_1 \approx \kappa_2$ which corroborates that $\delta(\text{Sphere(r)}) = \delta_{(\frac{1}{r}, \frac{1}{r})}$.

Notice that (we don't know if it is useful are not) you can estimate the radius minimum and maximum of the sphere particle only with the curvature diagrams and you can also estimate the mean radius of the sphere. This could have some application in medicine when size can give health information (in tumors for instance).

More precisely, the curvature diagram is obtained by first extracting the $2D$ mesh of the surface $u^{-1}(0)$ from the $3D$ volume u, by using the marching cubes algorithm [59]. The diffuse curvatures $k^\varepsilon_{1,u}, k^\varepsilon_{2,u}$ defined as :

$$\kappa^\varepsilon_1, u = \frac{H^\varepsilon_u + \sqrt{((H^\varepsilon_u)^2 - 4K^\varepsilon_u)^+}}{2}$$

$$\kappa^\varepsilon_2, u = \frac{H^\varepsilon_u - \sqrt{((H^\varepsilon_u)^2 - 4K^\varepsilon_u)^+}}{2}$$

where $x^+ = \max(0, x)$, are interpolated at the barycenter of each cell of the mesh. Then we get κ_1 and κ_2 and we plot them in the (κ_1, κ_2) axes.

As we saw, during lectures we then get a UMAP representation of textures for Wasserstein distance.

So this may have very interesting applications in medical fields. Since we know ([1]) that the texture is linked to the health of the cell/organism we are looking at, then we could compare and for predict wether or not we are facing with an ill cell/organism.

Notice that, we can also, in this space of histograms, distinguish bubble textures from tubular texture in a very efficient way.

We also thought that it is a way of pre-processing shape texture for clustering.

2 LIMITATIONS AND FUTUR POSSIBLE DIRECTION

Even if the boundary between the theoretical and the numerical is thin, we present here two possible research directions.

One idea that is given in the paper is to add the term $\int_S (n_S.\theta)^2 dS$ to the F functional, where n_S is the vector normal to S. This has the effect of orienting the tubes in a common direction and, overall, of ordering the structure of S in a certain sense.

This raises the question of how much control can be exercised over the characteristics of the resulting shape by knowing the formula for F. A question I find very interesting.

2.1 Theoritical side

A direction that seems to me very interesting but very difficult, (because a priori F_ε is neither linear nor convex nor derived from a norm) would be to show that

$$\inf_{\phi \in A} F_\varepsilon(\phi) \tag{8}$$

has at least one solution, where $A \subset \mathbb{R}^{\mathbb{R}}$ is correctly chosen to have compactness, for example.

One way of doing this would be to prove that $F_{varepsilon}$ is lsc, in which case by the theorem we have Γ convergence and therefore the existence of a minimizer.

In the literature, we find the following special cases where the existence of a minimizer is obtained:

(1) In [3] they have a existence results for $F_\varepsilon(\phi)$ associated to $a = (1, 2, 1, 0, 0, 0)$ and

$$A := W^{2,2}(\Omega) \cap \{ | \, |\phi|_{\partial\Omega} = 1, \nabla\phi \cdot \mathbf{n}_{\partial\Omega} = 0\}$$

(2) In [19], authors show that the problem of Cahn-Hilliard

$$\inf_{\phi \in \dot{H}^1} \int_\Omega \left(|\nabla\phi(x)|^2 + \frac{\varepsilon^2}{2} W(\phi(x)) \right) dx$$

has a solution. Where

$$A = \dot{H}^1(\Omega) := \left\{ f \in H^1(\Omega), \quad \int_\Omega f = 0 \right\}$$

The proofs relie on the fact that $u \mapsto ||\nabla u||$ is lse on $\dot{H}^1(\Omega)$. These arguments seem to be difficult to apply here.

(3) Concerning the Willemore functional some interesting results are obtained [28, 34, 35]

2.2 Numerical side

A.Song's paper [1] has inspired several other machine learning projects. More specifically, in [36], the authors use deep-learning methods to simulate shapes produced in [1] They use neural networks to learn how to generate sets of levels, with spectacular results.

Surprisingly, the Cahn-Hilliard equation has direct applications in imaging. This is the subject of this article [27]. The authors look at the problem of image reconstruction using the Cahn-Hilliard equation (modified, for $\lambda = 0$ we find the H^{-1} flow associated with $F_{varepsilon,\text{Cahn-Hilliard}}$), and obtain very promising results, [27].

Let $f(\mathbf{x})$, where $\mathbf{x} = (x, y)$, be a given image in a domain Ω, and suppose that $D \subset \Omega$ is the inpainting domain. Let $u(\mathbf{x}, t)$ evolve in time to become a fully inpainted version of $f(\mathbf{x})$ under the following equation:

$$\frac{\partial u}{\partial t} = -\Delta \left(\varepsilon \Delta u - \frac{1}{\varepsilon} W(u) \right) + \lambda(\mathbf{x})(f - u) \tag{1}$$

where

$$\lambda(\mathbf{x}) = \begin{cases} 0 & \text{if } \mathbf{x} \in D, \\ \lambda_0 & \text{if } \mathbf{x} \in \Omega \setminus D. \end{cases}$$

What about replacing (1) by the gradient flow generated by F ?

To conclude this research work, it should be pointed out that a very active area of research, from both a theoretical and numerical point of view, consists of coupling classical methods with Deep-Learning methods. There is still a huge amount of guaranteed theory and a great deal of numerical research to be explored.

Deep learning alone will not solve all the challenges, and even less so those linked to structure generation. Nevertheless, studies have shown that the combination of classical algorithms and deep learning yields unprecedented results.

Plus, there are very few theoretical guarantees [33] and mathematical frameworks that allow these neural networks to be studied. It is well known, for example, that Sobolev and Besov spaces suffer from the curse of dimensionality when it comes to solving PDEs numerically, [37].

For these reasons, other functional spaces have been introduced very recently [33] to enable their study.

This makes sense here, since in order to generate our Ω form, it is obtained as the zero of a function u which is the solution of a certain partial differential equation (6).

2.3 Two possible research directions

Can we use the functional spaces introduced in [33] to demonstrate the Γ convergence of $(F_\varepsilon)_{\varepsilon>0}$?

From an applied point view, let's take the example of a treatment for a rare disease. We'd like to simulate the effect of a drug using machine learning and computer vision methods. One of the major obstacles, which is the subject of ongoing research, is having enough data to train the algorithms. We could use this shape generation algorithm to enrich the training database of certain algorithms.

REFERENCES

[1] Anna Song, Journal of Mathematical Imaging and Vision 2021, *Generation of Tubular and Membranous Shape Textures with Curvature Functionals.*

[2] Kirstin Meyer, Hernan Morales-Navarrete, Sarah Seifert, Michaela Wilsch-Braeuninger, Uta Dahmen, Elly M Tanaka, Lutz Brusch, Yannis Kalaidzidis, Marino Zerial, *Bile Canaliculi Remodeling Activates YAP via the Actin Cytoskeleton During Liver Regeneration*, Molecular Systems Biology (2020) 16:e8985, https://doi.org/10.15252/msb.20198985.

[3] Qiang Du, Chun Liu, Rolf Ryham, and Xiaoqiang Wang, *A phase field formulation of the Willmore problem*, *Nonlinearity*, vol. 18, no. 3, pp. 1249–1267, 2005.

[4] Jean-Yves CHEMIN, *Bases of Functional Analysis*, Sorbonne Université, https://www.ljll.math.upmc.fr/chemin/pdf/2022_Poly_M1_VA_W.pdf.

[5] Evans, L.C., *Partial Differential Equations*, American Mathematical Society, Volume 19.

[6] Giovanni Bellettini and Luca Mugna, *Approximation of the Helfrich's Functional via Diffuse Interfaces.*

[7] Scikit-learn Python, *Scikit-learn*, https://scikit-learn.org/stable/index.html.

[8] Digital Library of Mathematical Functions, https://dlmf.nist.gov/10.22#E67.

[9] Roger, M., Schatzle, R., *On a Modified Conjecture of De Giorgi*, Mathematische Zeitschrift 254(4), 675–714 (2006).

[10] Bellettini, G., Mugnai, L., *Approximation of Helfrich's Functional via Diffuse Interfaces*, SIAM Journal on Mathematical Analysis.

[11] V. Subbiah, *The next generation of evidence-based medicine*, Nat Med, vol. 29, pp. 49–58, 2023. DOI: 10.1038/s41591-022-02160-z. URL: https://doi.org/10.1038/s41591-022-02160-z.

[12] Duarte, D., Hawkins, E.D., Akinduro, O., Ang, H., De Filippo, K., Kong, I.Y., Haltalli, M., Ruivo, N., Straszkowski, L., Vervoort, S.J., McLean, C., Weber, T.S., Khorshed, R., Pirillo, C., Wei, A., Ramasamy, S.K., Kusumbe, A.P., Duffy, K., Adams, R.H., Purton, L.E., Carlin, L.M., Lo Celso, C.: Inhibition of Endosteal Vascular Niche Remodeling Rescues Hematopoietic Stem Cell Loss in AML. Cell Stem Cell 22(1), 64–77.e6 (2018). DOI 10.1016/j.stem.2017.11.006. URL https://linkinghub.elsevier.com/retrieve/pii/S1934590917304587.

[13] T.J. Willmore, *Géométrie riemannienne*, Oxford University Press (1996).

[14] P.B. Canham, *The minimum energy of bending as a possible explanation of the biconcave shape of the human red blood cell*, Journal of Theoretical Biology 26(1), 61 – 81 (1970). DOI https://doi.org/10.1016/S0022-5193(70)80032-7. URL http://www.sciencedirect.com/science/article/ pii/S0022519370800327.

[15] W. Helfrich, *Elastic properties of lipid bilayers: theory and possible experiments*, Zeitschrift fur Naturforschung. Teil C: Biochemie, Biophysik, Biologie, Virologie 28(11), 693–703 (1973). DOI 10.1515/znc-1973-11-1209. URL https://doi.org/10.1515/znc-1973-11-1209.

[16] Thierry Biben, Klaus Kassner, Chaouqi Misbah, *Phase-field approach to three-dimensional vesicle dynamics*, Phys. Rev. E, vol. 72, no. 4, p. 041921, Oct 2005. DOI: 10.1103/PhysRevE.72.041921. URL: https://link.aps.org/doi/10.1103/PhysRevE.72.041921

[17] C. Gao, S. Peng, P. Feng, et al., *Bone biomaterials and interactions with stem cells*, *Bone Res*, **5**, Article 17059 (2017), https://doi.org/10.1038/boneres.2017.59.

[18] Chicco-Ruiz, A., Morin, P., Pauletti, M.S.: The shape derivative of the Gauss curvature. Revista de la Unión Matemática Argentina, pp. 311–337 (2018). DOI 10.33044/revuma.v59n2a06. URL http://inmabb.criba.edu.ar/revuma/revuma.php?p=doi/v59n2a06

[19] Craig Cowan, *The Cahn-Hilliard Equation as a Gradient Flow*, 2005.

[20] Doğan, G., Nochetto, R.H.: First variation of the general curvature-dependent surface energy. ESAIM: Mathematical Modelling and Numerical Analysis 46(1), 59–79 (2012). DOI 10.1051/m2an/2011019. URL http://www.esaim-m2an.org/10.1051/m2an/2011019

[21] G. Bellettini, L. Mugnai, *Approximation of Helfrich's Functional via Diffuse Interfaces*, SIAM Journal on Mathematical Analysis 42(6), 2402–2433 (2010). DOI 10.1137/09077549X. URL https://doi.org/10.1137/09077549X.

[22] Author: Maged Abdel-Kader, Ashraf Abulhamd, Abubaker Hamad, Abdullah Alanazi, Rizwan Ali, Saleh Alqasoumi Title: *Evaluation of the Hepatoprotective effect of combination between Hinokiflavone and Glycyrrhizin against CCl 4 induced toxicity in rats* Journal: *Saudi Pharmaceutical Journal* Volume: **26** Year: 2018 Month: 02 DOI: 10.1016/j.jsps.2018.02.009

[23] Web Site : urine-optmq-connexence,
title : Collecting Duct Renal Tubular Cells, http://urine.optmq.connexence.com/doceng/doc_036.html#:~:text=The%20collecting%20duct%20renal%20tubular%20cells%20are%20originally%20of%20a%2C%20nuclear%20membrane)%20and%20usually%20centric.,

[24] Author: John Jumper, Richard Evans, Alexander Pritzel, et al. Title: *Highly accurate protein structure prediction with AlphaFold* Journal: *Nature* Volume: **596** Pages: 583–589 Year: 2021 DOI: 10.1038/s41586-021-03819-2 URL: https://doi.org/10.1038/s41586-021-03819-2

[25] A. Henrot and M. Pierre, *Variation et optimisation de formes: une analyse géométrique*, Springer, 2005, Volume 48

[26] Francesco Maggi, *Sets of Finite Perimeter and Geometric Variational Problems*

[27] Andrea Bertozzi, Selim Esedoglu, Alan Gillette, *Inpainting of Binary Images Using the Cahn–Hilliard Equation*, IEEE Transactions on Image Processing, vol. 16, pp. 285–291, February 2007. DOI: 10.1109/TIP.2006.887728.

[28] Andrea Mondino and Christian Scharrer, *A strict inequality for the minimization of the Willmore functional under isoperimetric constraint*, May 6, 2021.

[29] S.V. Buldyrev. *Fractals in Biology*. In: Meyers, R. (eds) Encyclopedia of Complexity and Systems Science. Springer, New York, NY. 2009. https://doi.org/10.1007/978-0-387-30440-3_222

[30] L. Modica and S. Mortola, *Un esempio di Gammaconvergenza*, *Bollettino della Unione Matematica Italiana*, **14**, 285–299 (1977).

[31] G. Bellettini and M. Paolini, *Approssimazione variazionale di funzionali con curvatura*, *Seminario Analisi Matematica Univ. Bologna*, pp. 87–97 (1993).

[32] R. Röger and R. Schätzle, *On a Modified Conjecture of De Giorgi*, *Mathematische Zeitschrift*, **254**(4), 675–714 (2006). https://doi.org/10.1007/s00209-006-0002-6

[33] Weinan E, Chao Ma, Lei Wu. The Barron Space and the Flow-induced Function Spaces for Neural Network Models, *arXiv preprint arXiv:1906.08039, 2021.*

[34] Manuel Schlierf, *On the convergence of the Willmore flow with Dirichlet boundary conditions.*

[35] T. Rivière, *Variational principles for immersed surfaces with L2-bounded second fundamental form*, Preprint, 2010.

[36] Yaqi Guo, Saurav Sharma, Siddhant Kumar. *Inverse designing surface curvatures by deep learning*. arXiv preprint arXiv:2309.00163, 2023.

[37] Bellman, R. E., *Dynamic Programming (Princeton University Press, 1957),*